Primordial black hole production during first-order phase transitions

Jing Liu[1,2,*] Ligong Bian[3,4,†] Rong-Gen Cai,[5,2,1,‡] Zong-Kuan Guo[5,2,1,§] and Shao-Jiang Wang[5,‖]

[1]*School of Fundamental Physics and Mathematical Sciences, Hangzhou Institute for Advanced Study,*
University of Chinese Academy of Sciences, Hangzhou 310024, China
[2]*School of Physical Sciences, University of Chinese Academy of Sciences,*
No.19A Yuquan Road, Beijing 100049, China
[3]*Department of Physics, Chongqing University, Chongqing 401331, China*
[4]*Chongqing Key Laboratory for Strongly Coupled Physics, Chongqing University,*
Chongqing 401331, China
[5]*CAS Key Laboratory of Theoretical Physics, Institute of Theoretical Physics,*
Chinese Academy of Sciences, P.O. Box 2735, Beijing 100190, China

A novel mechanism for the primordial black hole (PBH) production is proposed as a natural and inevitable consequence of general first-order phase transitions without reference to specific underlying particle physics models. We obtain mutual predictions and constraints between primordial black holes and gravitational waves from phase transitions in the general case. For particular interest, our PBHs generated during a PeV-scale phase transition could make up all the dark matter, while PBHs generated during a MeV-scale phase transition could simultaneously account for LIGO-Virgo coalescence events and NANOGrav 12.5-yr result for the corresponding gravitational waves.

I. INTRODUCTION

The detection of gravitational waves (GWs) from the early Universe opens a new window to probe new physics [1,2]. Among them, the first-order phase transitions (PTs) are well motivated and predicted by many extensions of the Standard Model of particle physics (see, for example, [3] for a recent summary.) During a PT, the vacuum bubbles copiously nucleate due to quantum tunneling [4,5] and continuously release the vacuum energy into bubble walls and background plasma [6–8]. As the vacuum pressure pushes bubble walls forward, true vacuum bubbles continuously expand and finally collide with each other, generating large energy density perturbations and then produce GWs.

Furthermore, it has been proposed that the collapse of false vacuum bubbles formed during bubble collisions with a certain bubble-formation rate leads to the formation of primordial black holes (PBHs) [9–13]. PBHs are of broad interest for the ability to constitute even all dark matter [14,15] and explain the coalescence events observed by LIGO-Virgo collaboration [16,17]. Generally speaking, amplified energy density perturbations also provide the necessary conditions of PBH formation when generating

GWs. Once energy density fluctuations reach the threshold, PBHs formed from the gravitational collapse of the whole mass within a Hubble horizon [18,19]. In this paper, we propose a novel and generic mechanism of PBH formation during PTs arising from the asynochronization of the vacuum tunneling progress, which is different from the PBH formations mechanism proposed in Refs. [20–22] that proceeding through the collapse of fermion bubbles depending on the interaction between the scalar field and background plasma [20–22].

In this paper, we do not assume any specific particle physics model for PT to achieve such a PBH production channel, and find the PBH formation is a universal consequence of PTs. Because of the asynochronization of the vacuum tunneling progress, there always exist some Hubble-sized regions where the decay of the false vacuum is postponed. Since the radiation energy density decreases in the expanding Universe while the vacuum energy remains constant, the postpone of false vacuum decay leads to an increase in total energy density within those regions. At the time the vacuum energy inside those regions totally decays into other components, the overdensity reaches the maximum and the whole mass inside those regions may collapse into PBHs. Different from the previous works, we utilize the concrete numerical result of gravitational collapse [23,24] to obtain the exact result of the PBH abundance in terms of the basic model parameters of PTs, where numerical relativity simulation results are indispensable to obtain correct PBH formation mechanism.

[*]liujing@ucas.ac.cn
[†]lgbycl@cqu.edu.cn
[‡]cairg@itp.ac.cn
[§]guozk@itp.ac.cn
[‖]schwang@itp.ac.cn

Especially PBHs abundantly form in a relatively slow and supercooled PT. We also discuss the mutual constraints on GW energy spectrum and PBH abundance basing on our mechanism. For convenience, we choose $c = 8\pi G = 1$ throughout this paper.

II. PBHs FROM PTs

The exponential nucleation rate of vacuum bubbles reads [4,25]

$$\Gamma(t) = \Gamma_0 e^{\beta t}, \tag{1}$$

where Γ_0 is the initial value, the key parameter $\beta \geq 0$ represents the increasing rate. For the case $\beta \gg 1$, β^{-1} is also an estimation of the duration time of PTs. The averaged spatial fraction of the false vacuum reads [26]

$$F(t) = \exp\left[-\frac{4\pi}{3} \int_{t_i}^{t} dt' \Gamma(t') a^3(t') r^3(t, t')\right], \tag{2}$$

where $r(t, t') \equiv \int_{t'}^{t} a^{-1}(\tau) d\tau$ denotes the comoving radius of the true vacuum bubble and t_i is the nucleation time of the first bubble. Before t_i the false vacuum covers the whole space so $F(t) = 1$, and then $F(t)$ gradually decreases with the expansion of true vacuum bubbles. As $F(t)$ decreases, the vacuum energy is released to bubble walls and background plasma. The Friedmann equation reads

$$H^2 = \frac{\rho_v + \rho_r + \rho_w}{3}, \tag{3}$$

where ρ_v, ρ_r, and ρ_w are the energy densities of false vacuum, background radiation, and bubble walls, respectively. Here $\rho_v = F(t)\Delta V$ and ΔV is the energy density difference between the true and false vacua, where we have normalized the true vacuum energy density to be the zero point of the vacuum energy. $\alpha(t) \equiv \Delta V / \rho_r(t)$ is another key parameter that represents the ratio of the vacuum energy density released to the radiation bath during PTs. The initial value of $\alpha(t)$ determines the strength of the PT which is given later in specific cases. We assume the velocity of bubble walls is close to the speed of light. Thus, the equation of state parameters of both bubble walls and background plasma are $1/3$. Then, the evolution of radiation energy density reads

$$\frac{d(\rho_r + \rho_w)}{dt} + 4H(\rho_r + \rho_w) = \left(-\frac{d\rho_v}{dt}\right), \tag{4}$$

where the lhs represents the Hubble expansion effect and the rhs comes from the release of vacuum energy. Since the vacuum decay is probabilistic, there always exists some probability that in some Hubble volumes the vacuum decay is postponed, and the corresponding probability is obtained from Eq. (1),

$$P(t_n) = \exp\left[-\frac{4\pi}{3} \int_{t_i}^{t_n} \frac{a^3(t)}{a^3(t_{PBH})} H^{-3}(t_{PBH}) \Gamma(t) dt\right], \tag{5}$$

where t_n is the time for bubbles starting to nucleate in those Hubble volumes with postponed vacuum decay and t_{PBH} is the PBH formation time.

In the expanding Universe ρ_v is constant but $\rho_w, \rho_r \propto a^{-4}(t)$, so the delay of vacuum decay results in an increase of the total energy density. The energy density ratio inside and outside those regions, $\rho_{inside}/\rho_{outside}$, continues increasing until vacuum energy totally decays inside the overdense regions. At that time, $\rho_{inside}/\rho_{outside}$ reaches the maximum and remains a constant afterwards. Then, the mixture of both radiation and relativistic bubble walls collapse into PBHs if the overdensity reaches the threshold $1 + \delta_c$. Increasing t_n results in larger $\rho_{inside}/\rho_{outside}$ so that PBHs can form more easily. However, as implied by Eq. (5), the probability of the overdense regions quickly decreases with larger t_n, and the PBH abundance becomes smaller. Equation (5) also implies that $P(t_n)$ exponentially decreases with β. In other words, although PBHs naturally form during PTs, they can constitute a non-negligible part of dark matter only for relatively slow PTs.

If the energy density in one Hubble volume exceeds the critical density for a certain threshold, $\delta_c = 0.45$ [23,24], almost the whole mass in the Hubble horizon will collapse into a PBH, and the PBH mass reads

$$M_{PBH} \approx \frac{4\pi}{3} \gamma H^{-3}(t_{PBH}) \rho_c = 4\pi \gamma H^{-1}(t_{PBH}), \tag{6}$$

where ρ_c is the critical density and $\gamma \lesssim 1$ is a factor depending on detailed dynamics of gravitational collapse. See Ref. [27] for a more accurate estimation of the PBH mass, we simply adopt Eq. (6) as an illustration. In the next section, we will show the evolution of $\rho_v(t)$ and $\rho_r(t) + \rho_w(t)$, the amplification of energy density perturbations, as well as the predicted PBH mass function in detail.

The previous analysis implies that the PBH abundance only depends on the basic parameters α and β, and we do not assume any details of specific models. Thus, the mechanism and result of this work are generic.

In general, The PTs happen in the radiation-dominated era, and the scale factor a increases for many orders of magnitude until the time of matter-radiation equality. Since the PBHs energy densities $\rho_{PBH} \propto a^{-3}$ and radiation energy density $\rho_r \propto a^{-4}$, the proportion of PBH energy density is immensely amplified by the expansion of the Universe. Thus, the PBH abundance is non-negligible although the probability $P(t_n)$ may be many orders of magnitude smaller than 1.

III. THE PBH MASS FUNCTION AND GW ENERGY SPECTRUM

We consider two typical cases as examples: (1) a strong PT with $\alpha > 1$ and (2) a weak PT with $\alpha < 1$, and we give the evolution of each component of the energy density,
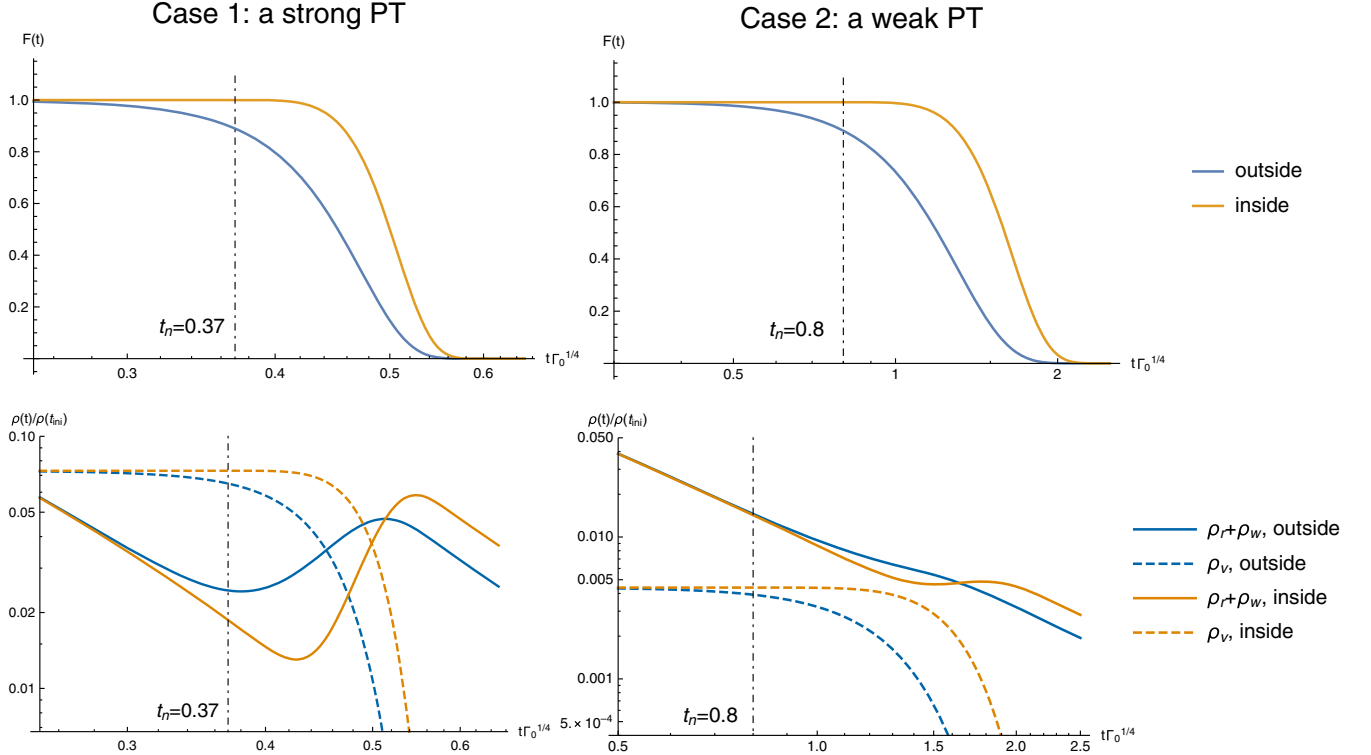
FIG. 1.   The evolution of the false vacuum fraction $F(t)$ (upper) and each component of the energy density (lower) in case 1 (left) and case 2 (right). The energy density of each component is rescaled by the initial value $\rho(t_i)$. The blue and orange lines denotes the conditions inside and outside the overdense regions. The dot-dashed line denotes the time of the first bubble nucleation t_n inside the overdense region. The solid and dashed lines in the lower panel, respectively, depict the evolution of the energy density of the false vacuum and the radiation.

then obtain the predicted GW energy spectrum and PBH abundance.

For the parameters we consider in the following, bubble collisions dominate the GW sources, and we neglect GWs from sound waves and magnetohydrodynamic turbulence. The numerical simulations under envelope approximation give the energy spectrum of GWs from bubble collisions[1] [28,29]

$$\Omega_{\mathrm{GW}}h^2(f) = 1.67 \times 10^{-5}(H_*/\beta)^2 \left(\frac{\kappa\alpha_*}{1+\alpha_*}\right)^2$$
$$\times \frac{0.11 v_w^3}{0.42 + v_w^2} \frac{3.8(f/f_p)^{2.8}}{1 + 2.8(f/f_p)^{3.8}}, \quad (7)$$

where v_w is the bubble wall velocity and we simply choose $v_w = 1$, κ is the fraction of energy density transferred from vacuum into bubble walls, the subscript $*$ denotes the parameters evaluated at the PT time, i.e., $F(t_*) = 0.7$ [30,31]. The peak frequency f_p reads

---

[1]The collapse of PBHs may result in additional GW production. Since the overdense regions are very rare in the whole Universe, this stochastic gravitational wave background (SGWB) is too weak compared to that sourced from bubble collisions elsewhere.

$$f_p = \frac{0.62}{1.8 - 0.1 v_w + v_w^2}(\beta/H_*)\frac{T_*}{100 \text{ GeV}}$$
$$\times 1.65 \times 10^{-5} \text{ Hz}, \quad (8)$$

where T_* is the PT temperature.

To obtain the evolution of the energy density, we solve Eqs. (1)–(4) together self-consistently assuming $t_i = 0$. In case 1, we choose $\beta/H_* = 14.8$, $\alpha_* = 6$, and $\kappa \to 1$. In case 2, we choose $\beta/H_* = 3.7$, $\alpha_* = 0.5$, $\kappa = 1/3$. Figure 1 shows the evolution of the false vacuum fraction $F(t)$ (upper) and each component of the energy density (lower) in case 1 (left) and case 2 (right), we can find that as $F(t)$ decreases, $\rho_r(t) + \rho_w(t)$ increases correspondingly, which means the vacuum energy transfers into bubble walls and background plasma. Comparing the blue and orange lines in each panel of Fig. 1, the decrease of $F(t)$ is postponed for t_n, since ρ_r scales as a^{-4}, the postpone of vacuum decay finally results in an increase of radiation energy density. At the end of simulation, $\rho_{\mathrm{inside}}/\rho_{\mathrm{outside}}$ exceeds the threshold $1 + \delta_c = 1.45$ and PBHs form.

The PBH abundance depends on α_* and β/H_*. For smaller α_*, Eq. (4) implies the quantum decay in the overdense region should be postpone to a larger t_n to reach the threshold δ_c, then the probability $P(t_n)$ decreases.
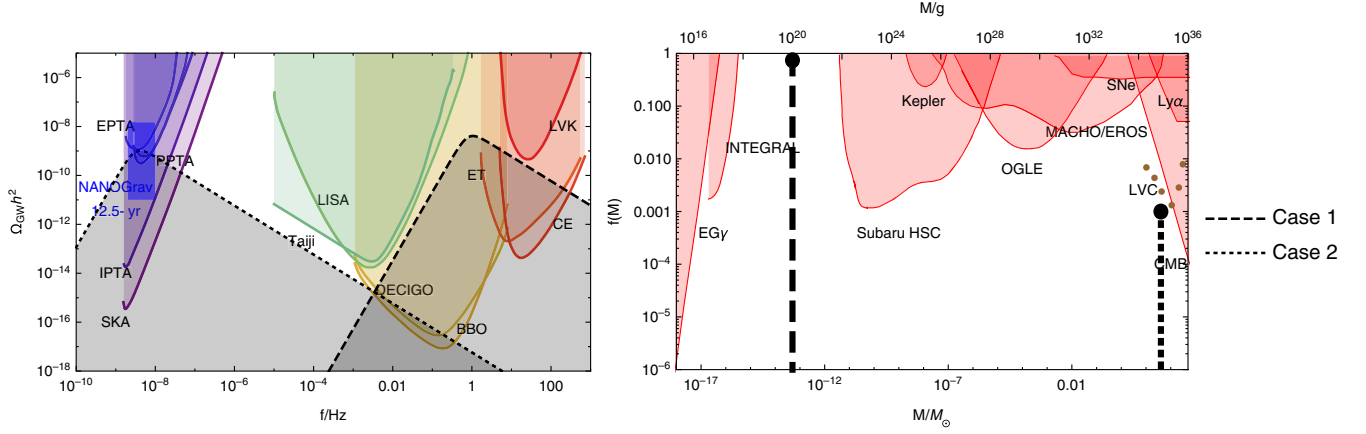
FIG. 2. The predicted GW energy spectra and PBH mass functions in each case. The sensitivity curves can be found in Ref. [38], including EPTA [39], PPTA [40], NANOGrav [41], IPTA [42], SKA [43], LISA [44], Taiji [45], DECIGO [46], BBO [47], LIGO, Virgo, and KAGRA (LVK) [48,49], CE [50], and ET [51]. The PBH constraints include EGγ [52], INTEGRAL [53–55], Subaru HSC [56], Kepler [57], OGLE [58], MACHO/EROS [59,60], SNe [61], Lyα [62], CMB [63], and LIGO-Virgo collaboration (LVC) [64].

For larger β/H_*, Equation (5) implies $P(t_n)$ decreases with t_n unchanged. Thus, the PBH abundance increases with α_* and decreases with β/H_*, while the PBH mass only depends on T_* according to Eq. (6).

The PT temperature in cases 1 and 2 are chosen to be $T_* = 1.58 \times 10^6$ GeV and $T_* = 28.6$ MeV, which are inspired from Peccei-Quinn axion models [32] and hidden sector models [33], respectively. In case 1 we choose $\gamma = 1$, PBHs with mass 10^{20} g constitute all dark matter and the predicted GW energy spectrum peaks at $f_p = 0.65$ Hz with the peak value $\Omega_{\mathrm{GW},p} = 4.3 \times 10^{-9}$, which are expected to be detected by DECIGO, BBO, ET, and CE, satisfying the current constraint by LIGO-Virgo collaboration [34]. In case 2 the predicted GW energy spectrum peaks at $f_p = 4 \times 10^{-9}$ Hz with the peak value $\Omega_{\mathrm{GW},p} = 10^{-9}$, which successfully explains the common spectrum process detected by NANOGrav collaboration [35,36]. PBHs formed in case 2 with the parameter $\gamma = 1/5$, whose abundance is predicted to be $\rho_{\mathrm{PBH}}/\rho_{\mathrm{DM}} = 10^{-3}$, can explain the coalescence events observed by LIGO-Virgo collaboration [37]. Figure 2 shows the predicted GW energy spectrum (left) and PBH mass function (right) in each case. Note that the nearly monochromatic mass function is an approximation here. In principle, one needs to consider the detailed collapsing process and the evolution of PBHs to obtain the small width of the mass function.

IV. CONCLUSION AND DISCUSSION

In this paper, we consider a novel mechanism of PBH formation during PTs as a model-independent universal consequence. Based on the numerical result of the collapse threshold of the whole Hubble horizon, we obtain an exact result of the predicted PBH abundance, and the mass function is almost monochromatic. We investigate two typical cases as examples and find that (1) PBHs from a PT

could constitute all dark matter, and the predicted Ω_{GW} peaks at about 0.65 Hz, which is expected to be observed by DECIGO, BBO, CE, and ET. (2) GWs and PBHs produced from a PT could both explain the common-spectrum process observed by NANOGrav and the coalescence events observed by the LIGO-Virgo collaboration.

Based on the mechanism in this work, we can further realize a more accurate GW-PBH mutual constraint in the PT case. Roughly speaking, for the PT temperature $T_* < 5 \times 10^8$ GeV (so that the PBHs are not evaporated), $\Omega_{\mathrm{GW}} < 10^{-7}$ is ruled out by the overproduction of PBHs. Our mechanism can give constraints on PTs parameters at a higher energy scale comparing with that from the GW observation of LIGO-Virgo collaboration [34]. The upcoming GW detectors can also give strict constraints on PBHs from PTs.

For the models where $v_w \lesssim 1$, the results remains roughly the same. In the other models where the bubble wall interacts strongly with background plasma, v_w is then much smaller than the speed of light. We qualitatively conclude here that both the GW strength and the PBH abundance are largely reduced in this case, and leave the quantitative analysis for future work. Since the GW energy spectrum from PTs depends on other parameters such as v_w, the sound speed, and the interaction between bubble walls and background plasma, from GWs produced by bubble collisions and sound waves one cannot determine all of the PT parameters.[2] Thus, the observations of both

---

[2]From the analytical point of view, the envelope approximation [65,66], bulk flow model [67,68], and sound shell method [69,70] give the GW energy spectrum from bubble collisions and sound waves. References [71–75] conduct precise numerical simulations for GWs from PTs. The characteristic energy spectrum of GWs helps to distinguish PT models and determine model parameters [76,77].

PBHs and GWs can eliminate degeneracy and give more strict constraints on model parameters.

The PBH formation mechanism proposed in this paper does not suffer from the fine-tuning problem encountered in the case of PBH production from curvature perturbations. PBHs can be overproduced during strong and slow PTs which happened at a temperature $T_* > 10^9$ GeV. These PBHs then dominate the Universe before their evaporation time, and the Planck relics of Hawking radiation could also account for dark matter. For the low-scale PTs inspired by the axion models, GWs may be detected through the B-mode polarization in the cosmic microwave background, and supermassive black holes with 10^6 solar mass can also be produced for an $\mathcal{O}(100)$ keV-scale dark PT.

In this work, we consider the collapse of the overdense regions in the whole Hubble volume. However, small false vacuum bubbles are more common in the same situation. These bubbles tend to shrink into a very small region and the energy is then highly concentrated. The interactions become so violent that nonlinear evolution may arise in such a small region. One needs numerical relativity simulations to obtain the final fate of the false vacuum bubbles. Moreover, smaller PBHs may arise if one takes into account the PBHs from bubble collisions surrounding the overdense regions. Thus, the result of PBH mass function in this work is a conservative estimation and smaller PBHs may be more abundant.

We plan to consider the following aspects to obtain more accurate results. (1) The lattice simulations of PTs in the Friedmann-Robertson-Walker Universe can give more accurate results of Ω_{GW}. (2) In more realistic models, such as the results presented in numerical simulations [72–74],

the equation of state parameter is not exactly $1/3$ at the end of PT. This may be caused by the equation of state parameter of bubble walls for $v_w < c$, or the nonzero effective mass of the scalar field near the true vacuum. The threshold δ_c is smaller in this case as stated in Ref. [78], which results in larger PBH abundance. For this work's originality and physical meaning, these problems deserve more detailed research, which we leave for future work.

ACKNOWLEDGMENTS

[1] R.-G. Cai, Z. Cao, Z.-K. Guo, S.-J. Wang, and T. Yang, Natl. Sci. Rev. **4**, 687 (2017).

[2] L. Bian et al., Sci. China Phys. Mech. Astron. **64**, 120401 (2021).

[3] C. Caprini et al., J. Cosmol. Astropart. Phys. 03 (2020) 024.

[4] S. R. Coleman, Phys. Rev. D **15**, 2929 (1977); **16**, 1248(E) (1977).

[5] C. G. Callan, Jr. and S. R. Coleman, Phys. Rev. D **16**, 1762 (1977).

[6] J. R. Espinosa, T. Konstandin, J. M. No, and G. Servant, J. Cosmol. Astropart. Phys. 06 (2010) 028.

[7] J. Ellis, M. Lewicki, J. M. No, and V. Vaskonen, J. Cosmol. Astropart. Phys. 06 (2019) 024.

[8] R.-G. Cai and S.-J. Wang, J. Cosmol. Astropart. Phys. 03 (2021) 096.

[9] S. W. Hawking, I. G. Moss, and J. M. Stewart, Phys. Rev. D **26**, 2681 (1982).

[10] M. Crawford and D. N. Schramm, Nature (London) **298**, 538 (1982).

[11] H. Kodama, M. Sasaki, and K. Sato, Prog. Theor. Phys. **68**, 1979 (1982).

[12] M. C. Johnson, H. V. Peiris, and L. Lehner, Phys. Rev. D **85**, 083516 (2012).

[13] M. Yu. Khlopov, R. V. Konoplich, S. G. Rubin, and A. S. Sakharov, arXiv:hep-ph/9807343.

[14] B. Carr, F. Kuhnel, and M. Sandstad, Phys. Rev. D **94**, 083504 (2016).

[15] B. Carr and F. Kuhnel, Annu. Rev. Nucl. Part. Sci. **70**, 355 (2020).

[16] M. Sasaki, T. Suyama, T. Tanaka, and S. Yokoyama, Phys. Rev. Lett. **117**, 061101 (2016); **121**, 059901(E) (2018).

[17] S. Bird, I. Cholis, J. B. Muoz, Y. Ali-Hamoud, M. Kamionkowski, E. D. Kovetz, A. Raccanelli, and A. G. Riess, Phys. Rev. Lett. **116**, 201301 (2016).

[18] J. C. Niemeyer and K. Jedamzik, Phys. Rev. Lett. **80,** 5481 (1998).

[19] F. Kühnel, C. Rampf, and M. Sandstad, Eur. Phys. J. C **76,** 93 (2016).

[20] C. Gross, G. Landini, A. Strumia, and D. Teresi, J. High Energy Phys. 09 (2021) 033.

[21] M. J. Baker, M. Breitbach, J. Kopp, and L. Mittnacht, arXiv:2105.07481.

[22] K. Kawana and K.-P. Xie, Phys. Lett. B **824,** 136791 (2022).

[23] I. Musco, J. C. Miller, and L. Rezzolla, Classical Quantum Gravity **22,** 1405 (2005).

[24] T. Harada, C.-M. Yoo, and K. Kohri, Phys. Rev. D **88,** 084051 (2013); **89,** 029903(E) (2014).

[25] K. Enqvist, J. Ignatius, K. Kajantie, and K. Rummukainen, Phys. Rev. D **45,** 3415 (1992).

[26] M. S. Turner, E. J. Weinberg, and L. M. Widrow, Phys. Rev. D **46,** 2384 (1992).

[27] I. Musco, V. De Luca, G. Franciolini, and A. Riotto, Phys. Rev. D **103,** 063538 (2021).

[28] M. Kamionkowski, A. Kosowsky, and M. S. Turner, Phys. Rev. D **49,** 2837 (1994).

[29] S. J. Huber and T. Konstandin, J. Cosmol. Astropart. Phys. 09 (2008) 022.

[30] A. H. Guth and S. H. H. Tye, Phys. Rev. Lett. **44,** 631 (1980); **44,** 963E (1980).

[31] J. Ellis, M. Lewicki, and J. M. No, J. Cosmol. Astropart. Phys. 04 (2019) 003.

[32] R. D. Peccei and H. R. Quinn, Phys. Rev. D **16,** 1791 (1977).

[33] Z. Chacko, L. J. Hall, and Y. Nomura, J. Cosmol. Astropart. Phys. 10 (2004) 011.

[34] A. Romero, K. Martinovic, T. A. Callister, H.-K. Guo, M. Martnez, M. Sakellariadou, F.-W. Yang, and Y. Zhao, Phys. Rev. Lett. **126,** 151301 (2021).

[35] Z. Arzoumanian et al. (NANOGrav Collaboration), Astrophys. J. Lett. **905,** L34 (2020).

[36] L. Bian, R.-G. Cai, J. Liu, X.-Y. Yang, and R. Zhou, Phys. Rev. D **103,** L081301 (2021).

[37] H. Deng, J. Cosmol. Astropart. Phys. 04 (2021) 058.

[38] K. Schmitz, J. High Energy Phys. 01 (2021) 097.

[39] L. Lentati et al., Mon. Not. R. Astron. Soc. **453,** 2577 (2015).

[40] R. M. Shannon et al., Science **349,** 1522 (2015).

[41] Z. Arzoumanian et al. (NANOGRAV Collaboration), Astrophys. J. **859,** 47 (2018).

[42] G. Hobbs et al., Classical Quantum Gravity **27,** 084013 (2010).

[43] C. L. Carilli and S. Rawlings, New Astron. Rev. **48,** 979 (2004).

[44] P. Amaro-Seoane et al. (LISA Collaboration), arXiv:1702 .00786.

[45] W.-H. Ruan, Z.-K. Guo, R.-G. Cai, and Y.-Z. Zhang, Int. J. Mod. Phys. A **35,** 2050075 (2020).

[46] S. Kawamura et al., Classical Quantum Gravity **28,** 094011 (2011).

[47] S. Phinney, P. Bender, R. Buchman, R. Byer, N. Cornish, P. Fritschel, W. Folkner, S. Merkowitz, K. Danzmann, L. DiFiore et al., NASA Mission Concept Study (2004).

[48] J. Aasi et al. (LIGO Scientific Collaboration), Classical Quantum Gravity **32,** 115012 (2015).

[49] K. Somiya (KAGRA Collaboration), Classical Quantum Gravity **29,** 124007 (2012).

[50] D. Reitze et al., Bull. Am. Astron. Soc. **51,** 035 (2019).

[51] M. Punturo et al., Classical Quantum Gravity **27,** 194002 (2010).

[52] B. J. Carr, K. Kohri, Y. Sendouda, and J. Yokoyama, Phys. Rev. D **81,** 104019 (2010).

[53] W. DeRocco and P. W. Graham, Phys. Rev. Lett. **123,** 251102 (2019).

[54] R. Laha, Phys. Rev. Lett. **123,** 251101 (2019).

[55] B. Dasgupta, R. Laha, and A. Ray, Phys. Rev. Lett. **125,** 101101 (2020).

[56] H. Niikura et al., Nat. Astron. **3,** 524 (2019).

[57] K. Griest, A. M. Cieplak, and M. J. Lehner, Phys. Rev. Lett. **111,** 181302 (2013).

[58] H. Niikura, M. Takada, S. Yokoyama, T. Sumi, and S. Masaki, Phys. Rev. D **99,** 083503 (2019).

[59] R. A. Allsman et al. (Macho Collaboration), Astrophys. J. Lett. **550,** L169 (2001).

[60] P. Tisserand et al. (EROS-2 Collaboration), Astron. Astrophys. **469,** 387 (2007).

[61] M. Zumalacarregui and U. Seljak, Phys. Rev. Lett. **121,** 141101 (2018).

[62] R. Murgia, G. Scelfo, M. Viel, and A. Raccanelli, Phys. Rev. Lett. **123,** 071102 (2019).

[63] V. Poulin, P. D. Serpico, F. Calore, S. Clesse, and K. Kohri, Phys. Rev. D **96,** 083524 (2017).

[64] V. Vaskonen and H. Veerme, Phys. Rev. D **101,** 043015 (2020).

[65] A. Kosowsky and M. S. Turner, Phys. Rev. D **47,** 4372 (1993).

[66] D. J. Weir, Phys. Rev. D **93,** 124037 (2016).

[67] T. Konstandin, J. Cosmol. Astropart. Phys. 03 (2018) 047.

[68] R. Jinno and M. Takimoto, J. Cosmol. Astropart. Phys. 01 (2019) 060.

[69] M. Hindmarsh, Phys. Rev. Lett. **120,** 071301 (2018).

[70] M. Hindmarsh and M. Hijazi, J. Cosmol. Astropart. Phys. 12 (2019) 062.

[71] M. Hindmarsh, S. J. Huber, K. Rummukainen, and D. J. Weir, Phys. Rev. Lett. **112,** 041301 (2014).

[72] M. Hindmarsh, S. J. Huber, K. Rummukainen, and D. J. Weir, Phys. Rev. D **92,** 123009 (2015).

[73] D. Cutting, M. Hindmarsh, and D. J. Weir, Phys. Rev. D **97,** 123513 (2018).

[74] D. Cutting, E. G. Escartin, M. Hindmarsh, and D. J. Weir, Phys. Rev. D **103,** 023531 (2021).

[75] Y. Di, J. Wang, R. Zhou, L. Bian, R.-G. Cai, and J. Liu, Phys. Rev. Lett. **126,** 251102 (2021).

[76] C. Caprini et al., J. Cosmol. Astropart. Phys. 04 (2016) 001.

[77] R.-G. Cai, M. Sasaki, and S.-J. Wang, J. Cosmol. Astropart. Phys. 08 (2017) 004.

[78] I. Musco and J. C. Miller, Classical Quantum Gravity **30,** 145009 (2013).